arXiv:1605.04101v1 [cond-mat.mtrl-sci] 13 May 2016

Enhancement of electron hot spot relaxation in photoexcited plasmonic structures by thermal diffusion

F. Spitzer,[1] B.A. Glavin,[2] V.I. Belotelov,[3,4] J. Vondran,[1] I.A. Akimov,[1,5]
S. Kasture,[6] V. G. Achanta,[6] D.R. Yakovlev,[1,5] and M. Bayer[1,5]

[1] *Experimentelle Physik 2, Technische Universität Dortmund, D-44221 Dortmund, Germany*
[2] *Lashkaryov Institute of Semiconductor Physics, 03028 Kyiv, Ukraine*
[3] *Lomonosov Moscow State University, 119991 Moscow, Russia*
[4] *Russian Quantum Center, 143025 Skolkovo, Moscow Region, Russia*
[5] *Ioffe Institute, Russian Academy of Sciences, 194021 St. Petersburg, Russia*
[6] *Tata Institute of Fundamental Research, 400005, Mumbai, India*

We demonstrate that in confined plasmonic metal structures subject to ultra-fast laser excitation electron thermal diffusion can provide relaxation faster than the energy transfer to the lattice. This relaxation occurs due to excitation of nanometer-sized hot spots in the confined structure and the sensitivity of its optical parameters to the perturbation in these regions. Both factors become essential when the plasmonic resonance condition is met for both excitation and detection. A pump-probe experiment on plasmonic gold lattices shows sub-picosecond relaxation with the characteristic times well-described by a two-temperature model. The results suggest that dynamical optical response in plasmonic structures can be tuned by selection of the structural geometry as well as the choice of wavelength and polarization of the excitation and detection light.

PACS numbers: 73.20.Mf, 78.47.J-, 78.66.Bz, 78.67.Pt

Currently fundamental plasmonic effects are intensely studied in pure and hybrid metallic structures, which possess also huge potential for numerous applications ranging from development of efficient nanolasers with plasmonic cavities to photodynamic cancer treatment with plasmonic nanoparticles[1,2]. In this regard, elucidating and understanding the relaxation dynamics and heat dissipation in plasmonic elements after excitation by a femtosecond light pulse is essential[3]. In a homogeneous metal, hot electrons loose their energy by emission of phonons, following the ultrafast initial stage of photoexcited carrier thermalization by electron-electron scattering. At room temperature, in most metals phonon relaxation occurs on time scales of the order of a picosecond or less[4]. In nanopatterned plasmonic structures, however, the light absorption becomes strongly inhomogeneous in space and shows in particular hot spots. Similarly, the reflection and transmission coefficients depend strongly on the spatial distribution of temperature. As a result, the optical response of the photoexcited structure is determined not only by electron cooling through phonon emission, but also by redistribution of energy in space via electron thermal diffusion (ETD).

In this letter we demonstrate that in plasmonic structures ETD evolves on timescales comparable to or even shorter than phonon emission, modifying significantly the sub-ps cooling dynamics as manifested by the ultrafast optical response. Nanoplasmonic metal structures are typically embedded in an environment with low thermal conductivity, so that during times shortly after the optical excitation they behave as thermally isolated systems with a correspondingly decelerated heat removal. Nevertheless, we show that in plasmonic structures which support optical excitation of nanometer-sized hot spots, ETD becomes feasible on ultrafast sub-ps time scales and provides a decisive contribution to the electron relaxation. Our results suggest that dedicated selection of material and geometry of a confined plasmonic structure allows tuning of its dynamical optical response by controlling the ETD process parameters.

For the ETD studies we used a model system of a plasmonic nanostructure: lateral gold gratings on top of a dielectric garnet layer, as schematically shown in Fig. 1. These structures can be considered as plasmonic crystals (PCs) which support surface plasmon polaritons (SPPs). The grating period is comparable to the wavelength of light in the visible/near-infrared spectral range which allows coupling of the far field radiation to the SPPs and vice versa. The transmission spectra in Fig. 1(a) show clear resonances which correspond to propagating SPPs at the metal-air and metal-dielectric interfaces. The investigated PCs combine two prime features in a single structure: high tunability of the plasmonic resonances and heat confinement in each of the grating stripes. The tunability is achieved by variation of the incidence angle and proper choice of the polarization of the excitation light pulse. This enables one to generate different hot spot distributions within a stripe and to modify the ETD flow. The thermal isolation is ensured by deposition of the PC on the dielectric substrate with low thermal conductivity. Most of the results presented below were obtained for a structure with stripe width $d_x = 460$ nm, stripe height $d_z = 130$ nm, and grating period $a = 590$ nm. In addition, measurements were performed on structures with $d_x = 290$ nm, $d_z = 80$ nm, and $a = 400$ nm, to study the scaling of the ETD relaxation with the lateral PC size. Additional details on the PC parameters and sample preparation are given in Refs.[5,6].

For measuring the dynamics of the PC optical response to pulsed excitation we implemented a pump-probe technique based on a Ti-Sa oscillator with a repetition frequency of 80 MHz emitting a broad-band spectrum centered at 800 nm wavelength with a full width at half maximum of about 80 nm. The optical pulses were chirp-compensated before entering the sample, providing an overall time resolution below 40 fs. The pump beam hit the sample in the plane perpendicular to the slits, while the probe beam was incident in the slit plane. The incidence angles of the pump θ_1, and the probe θ_2, could be tuned by rotating the sample around the axis parallel to the slits. All measurements were done at room temperature (300 K). An example of a differential transmission transient $\Delta T(t)/T$ for $\theta_1 = \theta_2 = 17^\circ$ is shown in Fig. 1(b). The negative spike at zero delay is due to instantaneous non-linear response of the dielectric[7]. It is followed by a rapid rise of the transmission with a time constant of about 50 fs which is attributed to the dynamical response of the imaginary part of the dielectric function due to the hot electron thermalization by electron-electron scattering right after the excitation pulse. The subsequent decay of the differential transmission during about a ps is due to electron-phonon relaxation, affecting mainly the real part of the dielectric function. Finally, there is an offset A_0 which originates from an increase of the lattice temperature by the optical excitation. In the following we concentrate on the sub-ps dynamics and substract A_0 from the signals.

Fig. 2 summarizes the data for different excitation conditions with plasmonic probe. Fig. 2(a) compares two transients for which in one case the pump beam polarization is plasmonic (p-pol, SPPs are excited) and non-plasmonic in the other case (s-pol, no SPP excitation). By switching from plasmonic to non-plasmonic excitation we observe a strong decrease of the signal due to less efficient excitation of hot carriers, in agreement with our previous work[7]. However, the most striking feature is the observation of double exponential decays of the optical transmission change ΔT induced by the pump. We note that the transients scale linearly with pump excitation power (up to 0.1 mJ/cm^{-2}) which suggests that this behavior represents a linear response. In order to quantify the signal contributions we use the function

$$\Delta T(t)/T = A_1 \exp\left(-t/\tau_1\right) + A_2 \exp\left(-t/\tau_2\right), \tag{1}$$

to fit the decay with the first (second) term describing the slow (fast) component. Variation of polarization and

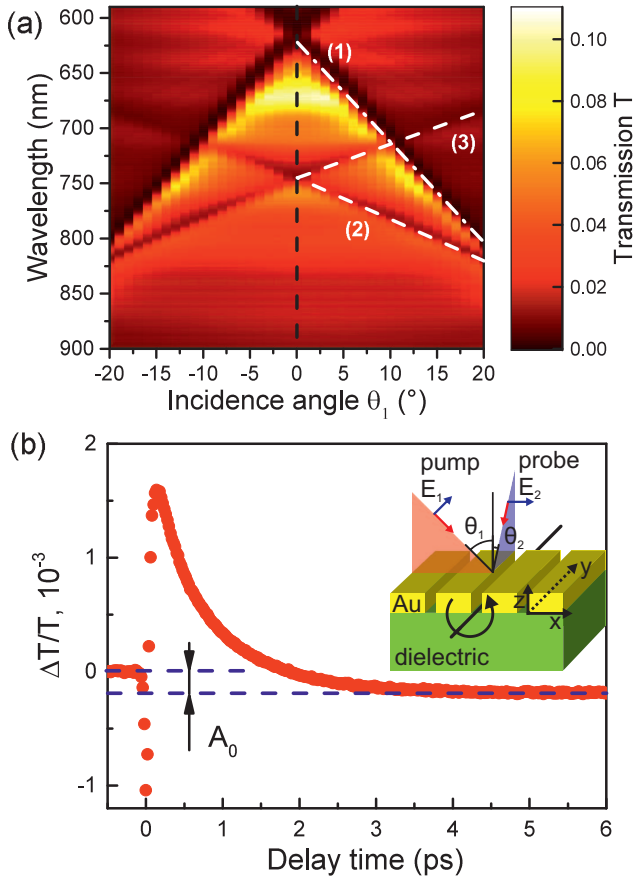

FIG. 1. (a) Contour plot of transmission T as function of wavelength and incidence angle θ_1 in PC with stripe width $d_x = 460$ nm. The spectra were taken with a white light source in p-pol. Dashed lines indicate SPP dispersion at Au-air (1) and Au-dielectric (2,3) interfaces. (b) Differential transmission transient $\Delta T/T$ measured at incidence angle of $\theta_1 = 17^\circ$ with p-polarized pump and s-polarized probe. Inset shows experimental geometry.

incidence angles of pump and probe results in changes of the amplitudes $A_{1,2}$ only, while the times $\tau_{1,2}$ remain constant for a given structure. In the PC with $d_x = 460$ nm fitting the experimental data provides $\tau_1 = 940$ fs and $\tau_2 = 300$ fs. Further, for plasmonic excitation A_2/A_1 is positive and strongly depends on the incidence angle. Otherwise, for s-polarized pump the ratio is negative and practically does not depend on θ_1 (see Fig. 2(b)). Similar measurements on the PC with $a = 400$ nm show a double-exponential decay with $\tau_1 = 940$ fs and $\tau_2 = 220$ fs.

The two-temperature model[11] used for analysis of the cooling dynamics and its manifestation in the pump-probe experiment are given in the appendix A. The evolution of the electron temperature T_e has a complex behavior which can be analyzed by decomposing the spatial distribution of T_e into the eigenmodes of the thermal problem. Each eigenmode is characterized by an individual relaxation time, resulting in general in a multi-exponential behavior. The amplitude weight of each eigenmode is determined by its contribution to the initial spatial distribution of T_e, initiated by the pump pulse. For the rectangular PC stripe, these eigenmodes are the harmonic Fourier components labeled by the indices n and m for the x- and z-directions (see appendix A). Their initial amplitudes B_{nm} are given by their overlap integrals with the initial distribution of T_e. For the perturbation of the optical transmission by the pump ΔT, we obtain

$$\Delta T = \frac{d\varepsilon}{dT_e} \sum_{n,m=0}^{\infty} k_{nm} B_{nm} \exp\left(-t/\tau_{nm}\right). \tag{2}$$

Here we assume that the perturbation of the dielectric function ε, which is proportional to the rise of T_e, is real, and k_{nm} are the perturbations of the transmission in response to the change of ε having the spatial structure of the (n, m) harmonic. The decay constant of each component $\tau_{nm}^{-1} = \tau_{eph}^{-1} + \frac{n^2}{\tau_x} + \frac{m^2}{\tau_z}$, where τ_{eph} is the time of electron energy relaxation due to phonon emission, and $\tau_{x,z} = C_e d_{x,z}^2 \pi^{-2} \kappa_e^{-1}$. Here κ_e and C_e are the thermal conductivity

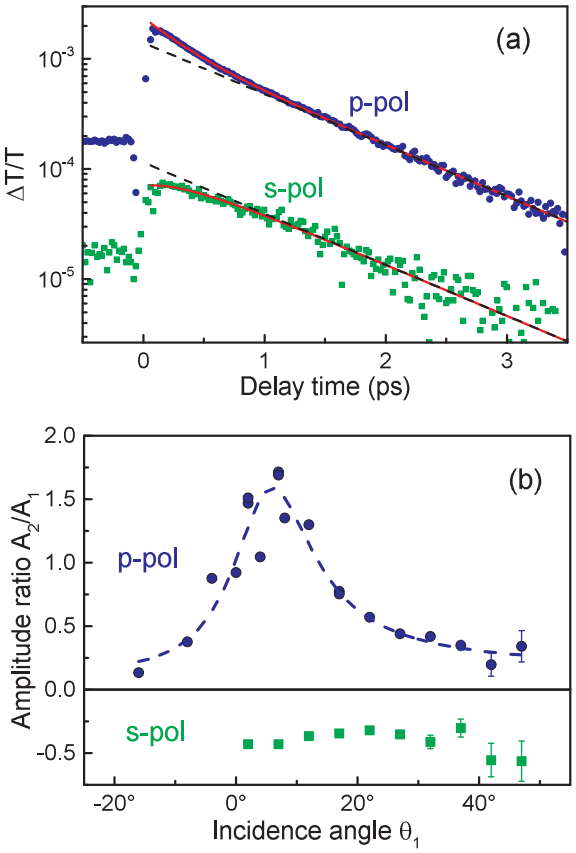

FIG. 2. (a) Differential transmission transients taken at $\theta_1 = 17^\circ$ for p- and s-polarized pump after substraction of A_0. Solid lines are fits with double exponential decay with $\tau_1 = 940$ fs and $\tau_2 = 300$ fs. (b) Dependence of A_2/A_1 on incidence angle θ_1 for the two polarizations. The data are presented for a PC with $d_x = 460$ nm. Dashed lines in (a) and (b) are guides to the eye.

and thermal capacity of the electrons, respectively. Note that Eq.(A12) reflects the main features of the relaxation process. The spectrum of relaxation times is determined by geometry and material of the structure and not directly related with its electromagnetic properties. On the other hand, optical access to a particular eigenmode depends on the possibility to couple the corresponding spatial profile of the perturbation to the laser radiation, both in excitation and detection. This coupling is determined by the plasmonic properties of the structure. It can be controlled by tuning wavelength, polarization and incidence angle of the laser. In our case, the plasmonic resonance enhances the amplitudes of particular harmonics with $n, m \neq 0$ such that they are comparable to the $n, m = 0$ contribution. If the probe is also in the plasmonic resonance band, its sensitivity to the spatially-inhomogeneous pattern may be enhanced for particular harmonics with $n, m \neq 0$.

The double exponential decay in Fig. 2 suggests that mostly two Fourier components contribute to the thermal perturbation. Let us provide some estimates in this respect. We assume $\kappa_e = 318$ WK^{-1}m^{-1}, $C_e = \gamma T_e$, and $\gamma = 68$ JK^{-2}m^{-3}[8,10], from which we obtain $\tau_x = 1.37$ ps, $\tau_z = 0.11$ ps. Obviously τ_z is very short and comparable to the electron scattering time[3]. This means that a thermal conduction approach can hardly be applied to modeling of the electron energy transfer along the z-direction. As we are interested in the electron relaxation after the initial stage lasting a few tens of fs, we can analyze the subsequent dynamics using the ETD approach solely for the x-direction considering the $m = 0$ harmonics. Another peculiarity of the PC is that even for finite incidence angle the pump excitation pattern is close to an even function of x with respect to the center of the stripe. As a result, the most important contributions arise from terms with even n, corresponding to even harmonics. From calculations of the amplitudes B_{nm} we conclude that the essential Fourier components are those with $n = 0$ and $n = 2$, both with $m = 0$. This is in line with the double-exponential behaviour in Fig. 2, so that we can identify $\tau_{1,2}$ with τ_{00} and τ_{02}. To obtain quantitative agreement with the measured values, we have to assume a somewhat reduced κ_e of about 250 WK^{-1}m^{-1}. This reduction may be caused by additional scattering of electrons at the surface and interfaces of

the stripes[12]. For the PC with $d_x = 290$ nm, theoretical and experimental values match for κ_e about 150 $\mathrm{WK^{-1}m^{-1}}$. The stronger reduction of κ_e in this case may be due to the smaller stripe thickness, enhancing the role of surface electron scattering.

The amplitudes $A_{1,2}$ deserve special attention. To that end, we show in Figs. 3(a) and (b) the spatial patterns of absorbed energy in a single stripe for plasmonic (p-pol, top) and non-plasmonic (s-pol, bottom) excitation. The bright areas indicate hot spot formation. The absorbed energy is proportional to $|\boldsymbol{E}|^2$, where $\boldsymbol{E}$ is the complex amplitude of the electric field vector of the optical pump wave in the metal from which the initial electron temperature distribution arises. The spatial distribution of $\boldsymbol{E}$ was calculated applying a rigorous coupled-wave analysis[13]. The excitation pattern for plasmonic polarization is shown for the incidence angle $\theta_1 = 17°$, which is close to the plasmonic resonance; for non-plasmonic excitation it is practically independent on θ_1.

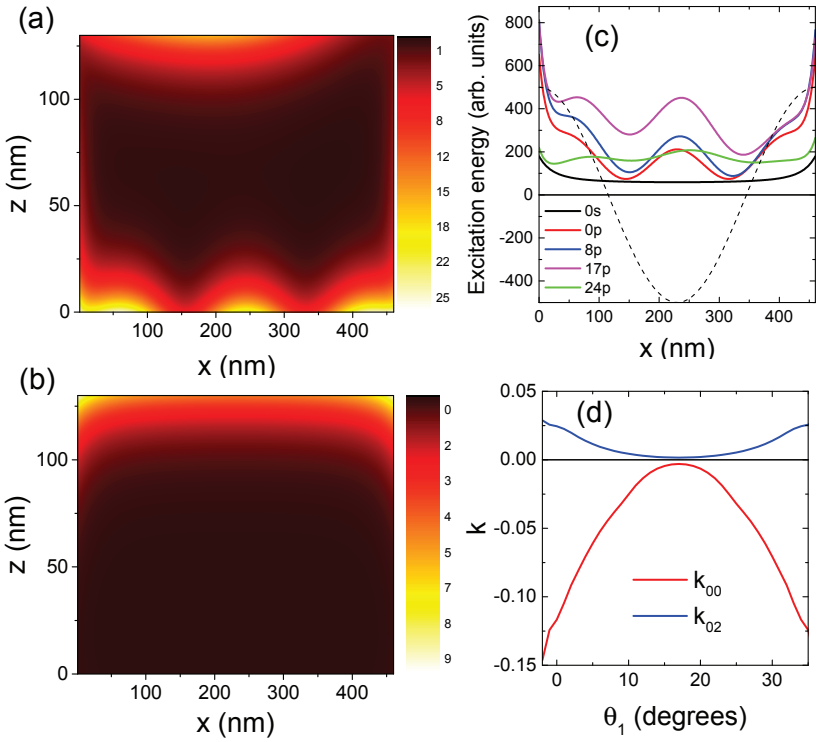

FIG. 3. (a) Contour plots of spatial distribution of the absorbed pump energy in PC stripe (arbitrary units). (a) and (b) correspond to excitation by p-polarized light ($\theta_1 = 17°$) and s-polarized light, respectively. Bright areas correspond to hot spots. In (c) the x-dependence of absorbed energy averaged over the z-direction is shown for various incidence angles at p-pol. and normal incidence for s-pol. For comparison also the harmonic with n=2 in the Fourier analysis of the thermal conduction problem, which provides fast relaxation with time constant τ_{02}, is shown. In (d) the angle dependence of coefficients k_{00} and k_{02} is shown.

For plasmonic excitation a pronounced hot spot structure is present scaling spatially with the wavelength of the uniform film SPPs, excited by the pump in the perforated structure. In Fig. 3(c) the absorbed energy (averaged over the z-direction) is shown for different incidence angles θ_1 demonstrating the absorption resonance for $\theta_1 = 17°$. The hot spots contribute considerably to the modes with $n \neq 0$. Obviously, the excitation spatial profile can not be described by the combination of the uniform, $n = 0$, and $n = 2$ harmonics (the latter is shown in Fig. 3(c) by the dashed line). However, for the harmonics with $n > 2$, τ_{nm} is very short. Similar to the case of vertical relaxation, the corresponding harmonics probably relax in a non-diffusive way being unresolvable for pump-probe delays exceeding a few tens of fs. For non-plasmonic excitation (shown for normal incidence only) the absorption is much weaker. However, also here hot spots are formed at the sharp edges of the rectangular stripes, which can be well described by the $n = 0$ and $n = 2$ terms in the Fourier series.

Next, we have to consider how the local variation of the dielectric fucntion translates into changes of transmitted probe intensity. The calculated angle dependencies of the coefficients k_{00} and k_{02} are shown in Fig.3(d). The results explain the negative sign of the ratio A_2/A_1 observed for non-plasmonic excitation. Indeed, the coefficients k_{00} and k_{02} have opposite signs for all considered angles. B_{00}, being the average absorbed excitation energy, is per se positive. Localization of the hot spots near the stripe edges for non-plasmonic pump ensures $B_{02} > 0$. For the plasmonic

	Au	Ag	Cu	Al	Ni	Pt	W	Fe
τ_{eph} (ps)	1	0.5	0.3	0.2	1	0.2	0.06	0.7
d_{th} (nm)	400	350	200	100	50	25	60	50

TABLE I. Electron-phonon cooling time and d_{th} for different metals. The material parameters are taken from[4,8–10]

configuration, we do not achieve quantitative agreement of experiment and theory. The experimental data suggest negative B_{02}, which would occur for intense hot spots in the middle of the stripes. They do appear in the calculations due to the excitation of the plasmonic resonance (see Fig. 3(a)), but the calculated hot spots near the wall edges provide larger contributions for incidence angles of $\theta_1 = 0$, 8, and 17°. Thus B_{02} should be positive there as well. According to our calculations, the absorbed energy near the edges is strongly sensitive to the stripe shape. Therefore, we tentatively attribute the discrepancy of experiment and theory to deviation of the stripe shape from the assumed rectangular one.

The developed model allows us to estimate the role of ETD also in plasmonic structures with a shape differing from a stripe and/or fabricated from a metal other than gold. ETD becomes important if its characteristic relaxation rate $\pi^2\kappa_e C_e^{-1} d^{-2}$, where d is the typical size of the hot-spot pattern in the plasmonic structure, is comparable to or exceeds τ_{eph}^{-1}. From setting the two rates equal, we can determine the required geometrical dimension of the plasmonic structure that needs to be undercut in order to reach these conditions, $d_{th} = \pi\sqrt{\kappa_e C_e^{-1} \tau_{eph}}$, which establishes a threshold for ETD becoming efficient. In table I we list the d_{th} as well as the τ_{eph} for various metals at 300 K. By tailoring material and geometry of the structure it is possible to obtain ETD relaxation faster than that due to phonon emission. In this case also shape design is important to provide a strongly inhomogeneous optical excitation pattern.

We would like to address the recent paper by Harutyunyan et al.[14] in which optical excitation of hot spots in plasmonic nano-discs was attributed to the appearance of a short optical response in differential reflection transients. However, the relaxation time constant could not be measured due to insufficient time resolution. Moreover, the role of ETD was not discussed as possible origin of the fast relaxation component.

In conclusion, we demonstrate that the relaxation in a photoexcited plasmonic grating can be enhanced by thermal diffusion of hot electrons on a sub-picosecond time scale, essentially below the value established for electron cooling by phonon emission. This fast relaxation is possible due to formation of nanometer-sized hot spots under ultra-fast optical excitation if the plasmonic resonance condition is met. Our analysis based on the two-temperature model provides good agreement with the experimentally observed relaxation times and allows us to formulate a geometric criterion for the importance of thermal diffusion which can be adjusted through the plasmonic structure material and design.

Appendix A: Theoretical consideration of thermal relaxation and transient optical response in metallic grating

Here, we theoretically consider the thermal relaxation of electrons in a metallic grating and the consequences on the transient optical response of the grating. The relaxation of photoexcited electrons in metals occurs in several stages. Commonly, the fastest stage implies thermalization of electrons resulting in a quasi-equilibrium electron distribution with the electron temperature exceeding that of the crystal lattice. This relaxation is due to efficient electron-electron scattering, and the corresponding times in metals are in the range of a few tens of fs (for gold, this value is claimed to be about 30 fs). Once thermalization is reached, the most universal process is cooling of electrons due to emission of phonons, i.e. transfer of the excess energy to the crystal lattice. For gold, the characteristic time of this process, τ_{eph} , is about 1 ps. For systems with a spatially inhomogeneous distribution of photoexcitation these processes are complemented by spatial electron energy transfer towards a balanced distribution. It has a quasi-ballistic character until electron thermalization is reached, switching to thermal diffusion afterwards. After the thermalization, the electron-lattice energy transfer can be described by the two-temperature model[11], which describes the electron-lattice energy balance where thermal diffusion occurs mainly due to electrons possessing superior thermal conductivity in comparison to the lattice. The underlying equations for electron and lattice tempearture variation with time are:

$$C_e \frac{\partial T_e}{\partial t} = \nabla \cdot (\kappa_e \nabla T_e) - G(T_e, T_l) + F(\boldsymbol{r}, t),$$
$$C_l \frac{\partial T_l}{\partial t} = G(T_e, T_l). \tag{A1}$$

Here $C_{e,l}$ are the electron and lattice heat capacity, κ_e is the electron heat conductivity, G is the electron-phonon coupling factor, and F describes the external power input into the electronic subsystem. The lattice thermal con-

ductivity is neglected. The common approximation valid for $T_{e,l}$ exceeding the Debye temperature is $G = g(T_e - T_l)$ with the temperature-independent g. In the linear-response regime, corresponding to small excitation fluence, we can neglect the temperature dependence of κ_e, $C_{e,l}$. It is important that in infinite or semi-infinite structures the thermal diffusion is not described by a characteristic time corresponding to an exponential decay, but rather obeys a power-like law. The situation is essentially different for spatially confined structures. Taking into account that the excitation of plasmonic structure takes place very fast, F can be assumed to be a δ-like function of time. The solution of Eq.(A1) can be written in terms of the initial electron temperature distribution $\Delta T_0(\boldsymbol{r})$. After simple algebra we obtain that this solution can be presented as a series

$$T_e = \sum_{n=0}^{\infty} \left(B_n^{(1)} \exp\left(-t/\tau_n^{(1)}\right) + B_n^{(2)} \exp\left(-t/\tau_n^{(2)}\right) \right) T_n(\boldsymbol{r}) \tag{A2}$$

$$T_l = \sum_{n=0}^{\infty} \left(\frac{B_n^{(1)}}{1 - \tau_{eph}/(\tau_n^{(1)}\xi)} \exp\left(-t/\tau_n^{(1)}\right) + \frac{B_n^{(2)}}{1 - \tau_{eph}/(\tau_n^{(2)}/\xi)} \exp\left(-t/\tau_n^{(2)}\right) \right) T_n(\boldsymbol{r}).$$

Here $\tau_{eph} = C_e/g$ is the electron-phonon energy relaxation time, $\xi = C_e/C_l$, and $T_n(\boldsymbol{r})$ are the eigenmodes of the Helmholtz equation

$$\nabla^2 T_n + q_n^2 T_n = 0 \tag{A3}$$

with the boundary condition of a zero gradient component of T_n normal to the surface, corresponding to the boundary condition of a thermally isolated structure. This problem provides eigenvalues q_n^2, each of which enter into the following two decay rates

$$\frac{1}{\tau_n^{(1,2)}} = \frac{1}{2} \left(\frac{1+\xi}{\tau_{eph}} + \frac{1}{\tau_n} \pm \sqrt{\left(\frac{1}{\tau_n} + \frac{1}{\tau_{eph}} \right)^2 - 2\xi \frac{1}{\tau_{eph}\tau_n} + \xi^2 \frac{1}{\tau_{eph}^2}} \right), \tag{A4}$$

where $\tau_n = \kappa_e (C_e q_n^2)^{-1}$ is the characteristic thermal diffusion relaxation time of the n-th mode. The coefficients $B_n^{(1,2)}$ are determined by the following expression:

$$B_n^{(1,2)} = \frac{B_n \tau_n^{(2,1)} (\xi \tau_n^{(1,2)} - \tau_{eph})}{(\tau_n^{(1,2)} - \tau_n^{(2,1)}) \tau_{eph}}, \tag{A5}$$

where the B_n are the coefficients in the expansion $\Delta T_0(\boldsymbol{r}) = \sum_n B_n T_n(\boldsymbol{r})$.

For metals usually $\xi \ll 1$. In this limit we obtain

$$\frac{1}{\tau_n^{(1)}} = \frac{1}{\tau_{eph}} + \frac{1}{\tau_n} \tag{A6}$$

$$\frac{1}{\tau_n^{(2)}} = \xi \frac{1}{\tau_{eph}} \left(1 - \frac{1}{2} \frac{\tau_n}{\tau_{eph} + \tau_n} \right)$$

$$B_n^{(1)} = B_n, B_n^{(2)} = -B_n \frac{\tau_n^{(1)}}{\tau_n^{(2)}}$$

These expressions reflect the fact that due to the big difference of electron and lattice heat capacities hot electrons, at the first stage, lose their energy due to phonon emission and thermal diffusion reaching a quasi-equilibrium state with the lattice. This stage is characterized by the times $\tau_n^{(1)}$. Then, much slower relaxation occurs on the time scale $\tau_n^{(2)}$, where both electron and lattice temperatures finally reach a uniform state. Since we are interested in the analysis of the fast stage of relaxation, we disregard the contributions of the $B_n^{(2)}$-terms to the electron temperature evolution.

Let us provide explicit results for the thermal relaxation within a stripe of a plasmonic grating. We chose the coordinate system such that the stripe is within the region $0 < z < d_z$, $0 < x < d_x$. From the general expressions for $\Delta T_0(x, z)$ we obtain

$$\Delta T_e \equiv T_e - T_l = \sum_{n,m=0}^{\infty} B_{nm} \exp\left(-t/\tau_{nm}\right) \cos\frac{\pi n x}{d_x} \cos\frac{\pi m z}{d_z}, \tag{A7}$$

where

$$\frac{1}{\tau_{nm}} = \frac{1}{\tau_{eph}} + \frac{n^2}{\tau_x} + \frac{m^2}{\tau_z},$$

$$\tau_{x,z} = \frac{C_e d_{x,z}^2}{\pi^2 \kappa}. \tag{A8}$$

The coefficients B_{nm} are determined by $\Delta T_0(x,z)$:

$$B_{nm} = \frac{\xi_n \xi_m}{d_x d_z} \int_0^{d_x} dx \int_0^{d_z} dz \Delta T_0(x,z) \cos\frac{\pi n x}{d_x} \cos\frac{\pi m z}{d_z}, \tag{A9}$$

with $\xi_i = 2$ for $i = 0$ and $\xi_i = 1$ otherwise. As we see the relaxation of nonequilibrium electrons has a multi-exponential character, with the exponents strongly dependent on the geometry of the structure (in the particular case of a stripe, on the dimensions of its cross-section). For actual structures $\tau_{x,z}$ can be as small as a few hundreds of fs.

The mechanism of the optical response to electron heating is based on perturbation of the metal dielectric permittivity by heating of the electrons[3]. In the linear response regime we can assume that this perturbation is proportional to ΔT_e. As a result, the perturbation of the dielectric perimittivity is given by

$$\Delta\varepsilon = \frac{d\varepsilon}{dT_e} \sum_{n,m=0}^{\infty} B_{nm} \exp\left(-t/\tau_{nm}\right) \cos\frac{\pi n x}{d_x} \cos\frac{\pi m z}{d_z}, \tag{A10}$$

where the derivative is calculated for ambient temperature. In general, it is a complex number, and we present it in the form $d\varepsilon/dT_e = \zeta \exp(i\varphi)$. To calculate the perturbation of the optical transmission of the system, ΔT_{opt}, we introduce the coefficients k_{nm}, defined as

$$k_{nm} = \frac{d\Delta T_{nm}}{d\varepsilon_{nm}}, \tag{A11}$$

where ΔT_{nm} is the perturbation of transmission induced by that of the dielectric permittivity $\varepsilon_{mn} \exp(i\varphi) \cos\frac{\pi n x}{d_x} \cos\frac{\pi m z}{d_z}$. In the linear response regime we have

$$\Delta T = \zeta \sum_{n,m=0}^{\infty} k_{nm} B_{nm} \exp\left(-t/\tau_{nm}\right), \tag{A12}$$

ACKNOWLEDGMENTS

The authors are grateful to Natalia Del Fatti and Fabrice Vallée for valuable discussions. The work was supported by the Deutsche Forschungsgemeinschaft (Projects ICRC TRR 160 and AK40/7-1), Volkswagen Foundation (Grant 90418), the Russian Foundation for Basic Research (Grant No. 16-02-01065), Russian President Grant (ID-5763.2015.2). VGA acknowledges Department of Science and Technology (DST), India.

[1] D.J. Bergman and M.I. Stockman, *Surface Plasmon Amplification by Stimulated Emission of Radiation: Quantum Generation of Coherent Surface Plasmons in Nanosystems*, Phys. Rev. Lett. **90**, 027402 (2003).

[2] M.L. Brongersma, N.J. Halas and P. Nordlander, *Plasmon-induced hot carrier science and technology*, Nat. Nanotechnol. **10**, 25 - 34 (2015).

[3] Fabrice Vallée and Natalia Del Fatti, *Ultrafast Nonlinear Plasmonics* Ch. 5 in *Plasmonics: Theory and applications*, ed. by T.V. Shahbazyan and M.I. Stockman, Springer, 2013.

[4] Z. Lin, L. V. Zhigilei, *Electron-phonon coupling and electron heat capacity of metals under conditions of strong electron-phonon nonequilibrium*, Phys. Rev. B **77**, 075133 (2008).

[5] V. I. Belotelov, I. A. Akimov, M. Pohl, V. A. Kotov, S. Kasture, A. S. Vengurlekar, Achanta Venu Gopal, D. R. Yakovlev, A. K. Zvezdin and M. Bayer, *Enhanced magneto-optical effects in magnetoplasmonic crystals*, Nat. Nanotechnol. **6**, 370 (2011).

[6] C. Brüggemann, A. V. Akimov, B. A. Glavin, V. I. Belotelov, I. A. Akimov, J. Jäger, S. Kasture, A. V. Gopal, A. S. Vengurlekar, D. R. Yakovlev, A. J. Kent, and M. Bayer, *Modulation of a surface plasmon-polariton resonance by subterahertz diffracted coherent phonons*, Phys. Rev. B **86**, 121401 (2012).

[7] M. Pohl, V.I. Belotelov, I.A. Akimov, S. Kasture, A.S. Vengurlekar, A.V. Gopal, A.K. Zvezdin, D.R. Yakovlev, and M. Bayer, *Plasmonic crystals for ultrafast nanophotonics: Optical switching of surface plasmon polaritons*, Phys. Rev. B **85**, 081401(R) (2012).

[8] David R. Lide, CRC Handbook of Chemistry and Physics (CRC Press, Florida, 2003).

[9] E. Carpene, E. Mancini, C. Dallera, M. Brenna, E. Puppin and S. De Silvestri, *Dynamics of electron-magnon interaction and ultrafast demagnetization in thin iron films*, Phys. Rev. B **78**, 174422 (2008).

[10] G. R. Stewart, *Measurement of low-temperature specific heat*, Rev. Sci. Instr. **54**, 1 (1983).

[11] S.I. Anisimov, B.L. Kopeliovich, and T.L. Perel'man, *Electron emission from metal surfaces exposed to ultrashort laser pulses*, Zh. Eksp. Teor. Fiz. **66**, 776 (1974) (Sov. Phys.- JETP **39**, 375 (1974)).

[12] G. Chen, P. Hui, *Thermal conductivities of evaporated gold films on silicon and glass*, Appl. Phys. Lett. **74**, 2942 (1999).
[13] M. G. Moharam, D. A. Pommet, E. B. Grann, and T. K. Gaylord, *Stable implementation of the rigorous coupled-wave analysis for surface-relief gratings: enhanced transmittance matrix approach*, J. Opt. Soc. Am. A **12**, 1077 (1995).
[14] H. Harutyunyan, A. B. F. Martinson, D. Rosenmann, L.K. Khorashad, L.V. Besteiro, A.O. Govorov, and G.P. Wiederrecht, *Anomalous ultrafast dynamics of hot plasmonic electrons in nanostructures with hot spots*, Nat. Nanotechnol. **10**, 770-774 (2015).